Journal of Applied Polymer Science

Graft copolymerization of methyl methacrylate from brominated poly(isobutylene-*co*-isoprene) via atom transfer radical polymerization

Jinyuan Wang,[1] Chaoying Wan,[2] Yong Zhang,[1] Yinghao Zhai,[1] Shiqiang Song,[1] Wentan Ren,[1] Zonglin Peng[1]

[1]School of Chemistry and Chemical Engineering, State Key Laboratory of Metal Matrix Composites, Shanghai Jiao Tong University, Shanghai 200240, China

[2]International Institute for Nanocomposites Manufacturing, WMG, University of Warwick, Coventry CV4 7AL, United Kingdom

Correspondence to: Y. Zhang (E-mail: yong_zhang@sjtu.edu.cn)

ABSTRACT: Commercial brominated poly(isobutylene-*co*-isoprene) (BIIR) rubber has been directly used for the initiation of atom transfer radical polymerization (ATRP) by utilizing the allylic bromine atoms on the macromolecular chains of BIIR. The graft copolymerization of methyl methacrylate (MMA) from the backbone of BIIR which was used as a macroinitiator was carried out in xylene at 85°C with CuBr/*N*,*N*,*N*′,*N*″,*N*″-pentamethyldiethylenetriamine as a catalytic complex. The polymerization conditions were optimized by adjusting the catalyst and monomer concentration to reach a higher monomer conversion and meanwhile suppress macroscopic gelation during the polymerization process. This copolymerization followed a first-order kinetic behavior with respect to the monomer concentration, and the number-average molecular weight of the grafted poly(methyl methacrylate) (PMMA) increased with reaction time. The resultant BIIR-*graft*-PMMA copolymers showed phase separation morphology as characterized by atomic force microscopy, and the presence of PMMA phase increased the polarity of the BIIR copolymers. This study demonstrated the feasibility of using commercial BIIR polymer directly as a macromolecular initiator for ATRP reactions, which opens more possibilities for BIIR modifications for wider applications. © 2016 Wiley Periodicals, Inc. J. Appl. Polym. Sci. **2016**, *133*, 43408.

KEYWORDS: atom transfer radical polymerization; butyl rubber; copolymers; grafting

Received 31 October 2015; accepted 4 January 2016
DOI: 10.1002/app.43408

INTRODUCTION

Poly(isobutylene-*co*-isoprene) or butyl rubber (IIR) containing isobutylene and ~2% of isoprene has played an important role in tire and adhesive industries due to its unique properties such as high damping properties, excellent ageing resistance, and low gas permeability.[1–4] However, its nonpolar polymer chains limit its interaction with other polar materials.[5,6] Thus, there has been a long-term interest in investigating the chemical modification of IIR to enhance its polarity and reactivity and broaden its applications. For example, IIR modified with sodium hydride and maleic anhydride via a solvent-free process has demonstrated increased curing rate due to the introduction of polar functional groups and double bonds.[7] Several new IIR-based macromonomers were reported by displacing bromide of brominated IIR (BIIR) with carboxylate nucleophiles in toluene, and higher cure extents were achieved using highly reactive pendant functional groups in the context of peroxide-initiated cross-linking.[8]

So far, various controlled radical polymerization approaches have been developed for preparing graft copolymers with controlled molecular structures and effectively avoiding macroscopic gelation.[9–12] Atom transfer radical polymerization (ATRP)[13,14] is an effective method for synthesis of graft copolymers using macroinitiators (grafting-from approach),[15–18] macromonomers (grafting-through approach)[19,20] or forming side chains (grafting-onto approach).[15,21,22] The "control" characteristic of ATRP is accomplished by maintaining an equilibrium between propagating radicals and dormant species via a reversible redox process by the addition of transition metal/ligand complexes in their low oxidation state,[23] so that ensures narrow molecular weight distribution and high terminal functionalities.

Commercial rubbers are of great interest as macroinitiators for the synthesis of new graft copolymers with controlled microstructure and properties nowadays. For example, Gillies *et al.*[24] synthesized carboxylic acid-functionalized IIR using ATRP method via introduction of poly(carboxylic acid) which involves the conjugation of 2-bromoisobutyryl groups as initiator. Truelsen *et al.*[25] prepared a macroinitiator from a triblock copolymer of polyisobutylene with end blocks of poly(*p*-methylstyrene) by bromination with 2-bromoisobutyryl bromide. Controlled

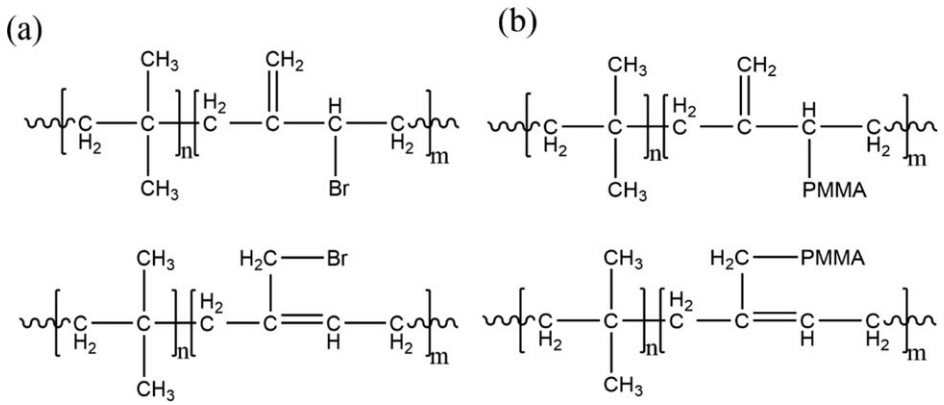

Scheme 1. Molecular structure of (a) BIIR and (b) BIIR-*g*-PMMA.

polymerization of styrene and *p*-acetoxystyrene yields new triblock copolymer structures with densely grafted end blocks. By using brominated ethylene–propylene–diene terpolymer (EPDM-Br) as a macromolecular initiator, methyl methacrylate (MMA) was successfully polymerized and grafted from EPDM forming EPDM-*g*-PMMA copolymers via ATRP. The maximum graft efficiency of 93% was obtained at 90°C for 20 h, with the ratio of EPDM-Br/CuBr/bpy of 1/0.8/2.4.[6] With chloromethylated polystyrene-*b*-poly(ethylene-*co*−1-butene)-*b*-polystyrene (SEBS-Cl) as a macroinitiator, Xu *et al.*[5] synthesized SEBS triblock copolymers by using activators generated by electron transfer (AGET) ATRP. Different kinds of graft copolymers SEBS-*g*-PMMA, SEBS-*g*-polystyrene, and SEBS-*g*-poly(butyl acrylate) with predetermined molecular weights and low polydispersity could be obtained. However, all the above reported reactions require expensive halogenation reagents.

In this work, without prebromination reaction, a commercial BIIR as a product of halogenated IIR made from a solution process using liquid bromine in a saturated hydrocarbon solvent,[26,27] was directly used as a macroinitiator for ATRP graft copolymerization. The BIIR as a macroinitiator contains primary and secondary allylic bromines with its macromolecular structure proposed in Scheme 1(a).[27–29] The synthesis of PMMA-grafted BIIR copolymers (BIIR-*g*-PMMA) can be challenging because the relatively high number-average molecular weight (M_n) around 270,000 of the BIIR macroinitiator may hinder the dispersion of MMA and the growth of PMMA chains from the BIIR backbones. In addition, because the initiation efficiency of allyl halide (macro)initiators is low[30] (the specific initiation efficiency of BIIR cannot be obtained from the ratio of theoretical M_n to actual M_n because the molecular weight of PMMA fragments neither can be directly determined as the PMMA side chains cannot be cleaved using an acidolysis reaction nor can be calculated by NMR as the brominated butyl rubber is actually a compound prepared from IIR containing small amount of isoprene, and only some of which has been brominated), it is very likely to cause inter- or intramolecular coupling reactions among the long-side-chain radicals, thus may form macroscopic gelation or cross-linking.[31,32] To avoid the gelation reaction and enhance the graft polymerization efficiency, a series of experiments have been conducted by investigating the effects of CuBr, $CuBr_2$, and monomer concentration on the reaction conditions.

EXPERIMENTAL PROCEDURE

Materials

BIIR (Bromobutyl 2030, $M_n \approx 270\,000$, allylic bromide content 1.8 wt %, i.e., 60 bromine per chain) was kindly supplied by Lanxess GmbH, Germany. It was purified by a solution-precipitation process to remove stabilizers (epoxidized soybean oil) and antioxidants, with hexane as solvent and acetone as precipitant, and dried in a vacuum oven at 60°C for 48 h.

Methyl methacrylate (MMA, 98%, Sinopharm Chemical Reagents Co. Ltd., China) was purified by passing through a column filled with basic alumina to remove inhibitors before use; xylene (97%, Sinopharm Chemical Reagents Co. Ltd, China) was distilled in the presence of CaH_2 to eliminate any traces of water and stored in the presence of 4 Å molecular sieve; and Copper(I) bromide (CuBr, 99.8%, Sinopharm Chemical Reagents Co. Ltd., China), Copper(II) bromide ($CuBr_2$, 99.8%, Sinopharm Chemical Reagents Co. Ltd., China), and *N*,*N*,*N*′,*N*″,*N*″-pentamethyldiethylenetriamine (PMDETA, 99%, Aladdin) were used as received.

Synthesis of BIIR-g-PMMA

In a typical polymerization, BIIR (1.110 g, 0.25 mmol initiating site) and xylene (40.000 g, 0.38 mol) were added to a dried 100 mL three-necked round-bottomed flask equipped with a magnetic stirring bar and sealed with rubber septum. After BIIR was fully dissolved, MMA (5.006 g, 50 mmol) was added. Then the mixture was bubbled by N_2 for 30 min followed by the addition of PMDETA (0.13 g, 0.75 mmol) and CuBr (0.036 g, 0.25 mmol). Finally the system was heated to 85°C in oil bath and kept bubbling N_2. At specified time intervals, samples were taken from the flask under an N_2 atmosphere using degassed syringes to calculate monomer conversion and determine molecular weight. After a period of time, the polymerization was stopped by removing the flask from the oil bath and opening the flask to expose catalysts to air. The resulting polymer was precipitated by pouring the reaction mixture into cold methanol. After separated, the precipitate was dissolved in THF, and precipitated into cold methanol for three times. The final product was dried overnight under vacuum at 60°C (1.83 g for 9 h of reaction, yield: 83.5%, the mass fraction of PMMA in the product of BIIR-g-PMMA calculated gravimetrically is about 0.39).

Table I. Reaction Condition Optimization of ATRP of MMA from BIIR Macroinitiator

Entry	M/I/CuBr/PMDETA	Time (h)	Conv[a] (%)
1[b]	400/1/1/3	0.4	Gel
2[b]	400/1/0.5/1.5	8	22.5
3[b]	400/1/0.75/3/0.25($CuBr_2$)	8	11.1
4[b]	200/1/1/3	0.4	Gel
5[b]	200/1/0.5/1.5	8	22.4
6[c]	200/1/1/3	8	29.5

[a] Conversion was obtained gravimetrically.
[b] Xylene/MMA = 4/1 (w/w); $T = 85$°C.
[c] Xylene/MMA = 8/1; $T = 85$°C.

Analytical Methods

Monomer conversion was calculated gravimetrically by drying to constant weight in a vacuum oven at 60°C.

Number-average molecular weight ($M_{n,GPC}$) and molecular weight distribution index (M_w/M_n) were estimated by using a gel permeation chromatography (GPC) with Perkin Elmer Series 200 equipped with PSS columns (5 μm PSS SDV gel, 10^2, 10^3, 10^4, and 10^5 Å, 30 cm each) and THF as eluent at a flow rate of 1.0 mL/min at room temperature, with detection by Waters 410 differential refractometer and Waters photodiode array detector operated at 254 nm. The column system was calibrated with narrow polystyrene (PS) standards (PSS, Mainz).

Attenuated total reflection-Fourier transform infrared (ATR-FTIR) spectra were acquired using Perkin Elmer Spectrum 100 spectrophotometer equipped with a single horizontal Golden Gate ATR cell. Four scans were acquired in the 4000–650 cm^{-1} range with a resolution of 0.4 cm^{-1}. The resulting graft copolymer after different time of reaction was isolated by solution-precipitation process with hexane as a solvent and acetone as a precipitant followed by extraction of acetone in Soxhlet extractor for 24 h to rule out PMMA.

Hydrogen nuclear magnetic resonance (^{1}H NMR) spectra were recorded in $CDCl_3$ as a solvent using a Bruker AVANCEIII 400 spectrometer. The resulting graft copolymer after different time of reaction was isolated by solution-precipitation process with hexane as solvent and acetone as precipitant followed by extraction of acetone in Soxhlet extractor for 24 h to rule out PMMA.

Thermal characteristics of the graft copolymers were determined by Differential scanning calorimetry (DSC) using TA Instruments model Q2000. The DSC measurements were performed on *ca* 8 mg sample in nitrogen atmosphere from −80 to 150°C at a scanning rate of 20°C/min.

The surface morphology of the graft copolymer films was observed on a Nanoscope IIIa scanning probe microscope (Digital Instruments, Santa Barbara, CA) mounted with silicon tips (125 μm in length and 500 kHz resonant frequency) in tapping mode under ambient conditions, and the scan frequency was 2.0 Hz. The precipitated graft copolymers were dissolved in THF to produce 1 mg/mL solutions. The films were prepared by spin coating on cleaned silicon wafer substrates using the dilute solutions of the copolymers. The wafers were rinsed thoroughly to remove any existing chemical or particulate contaminants, by a few minutes of ultrasonic treatment in ethanol and acetone, and then dried at 100°C. The copolymer films were annealed in THF vapors to improve the organization/orientation of the PMMA domains. For that purpose, the copolymer films onto their silicon wafers were placed in a closed glass vessels (40 × 25 mm^2 flat-type weighing bottle) at room temperature above (1 cm) a reservoir of solvent (3 mL). After 24 h of exposition, the silicon wafers were promptly took out from the vessel and dried at room temperature.

Static water contact angle (SWCA) was conducted on a contact angle measuring instrument (Kruss DSA30, Germany) at room temperature by using the sessile drop method. The presented SWCA of a film sample represented the average value obtained from at least five different locations. To prepare the film samples for SWCA, the polymers were compressed into a 0.2-mm-thick flat sheet using a Lebtech LP-S-50 hydraulic press at 180°C under a pressure of 10.4 MPa for 6 min.

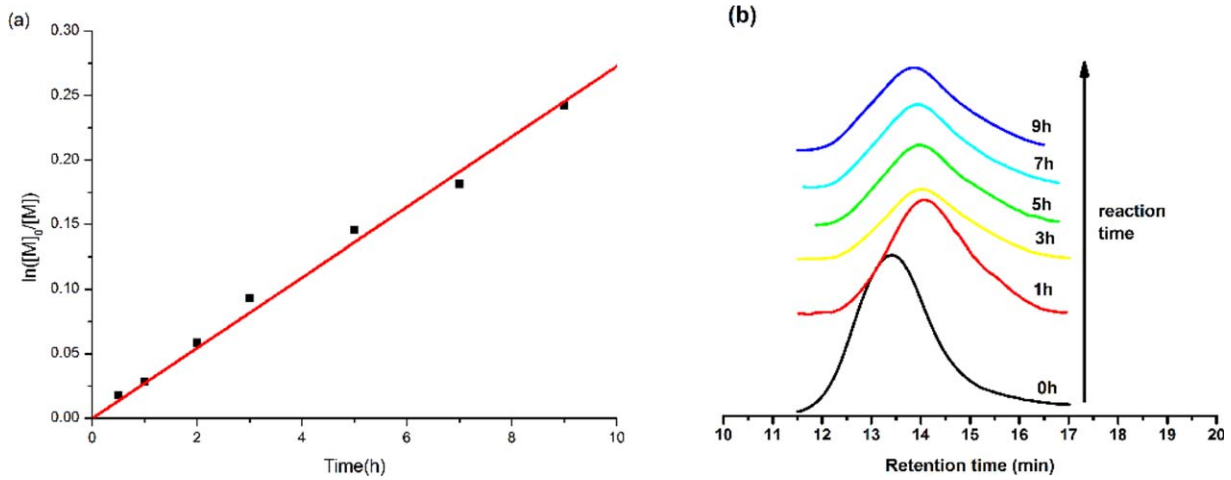

Figure 1. (a) Semilogarithmic plot of monomer conversion vs time and (b) GPC traces (with THF as eluent and calibrated using PS standard). Reaction condition: entry 6 of Table I. [Color figure can be viewed in the online issue, which is available at wileyonlinelibrary.com.]

Table II. Molecular Weight Parameters for the atRP of BIIR-*g*-PMMA at Different Reaction Time

Time (h)	Conv[a] (%)	$M_{n,theo}$[b] $\times 10^{-5}$	$M_{n,GPC}$[c] $\times 10^{-5}$	M_w/M_n[c]	DP_{theo}[d]	DP_{NMR}[e]	$f_{PMMA,NMR}$[f]
0	0	2.68	2.68	1.56	0	0	0
1	2.8	3.04	1.00	1.63	6	2	0.07
3	8.9	3.76	1.33	1.46	18	10	0.25
5	13.6	4.30	1.66	1.41	27		
7	16.6	4.66	2.05	1.37	33		
9	21.5	5.26	2.53	1.36	43	22	0.41

[a] Conversion was obtained gravimetrically.
[b] $M_{n,theo} = M_I + 60([M]_0/[I]_0) \times$ conversion $\times M_{monomer}$.
[c] M_w and M_n based on MALLS using THF as eluent and PS as standards, dn/dc = 0.1353 (BIIR).
[d] Degree of polymerization calculated by conversion.
[e] Degree of polymerization calculated by NMR based on average number of 60 initiated sites per BIIR chain assuming 100% initiation efficiency.
[f] The mass fraction of PMMA in the product of BIIR-*g*-PMMA calculated by from the ratio (*R*) of the peak area of the methylene group to that of the methoxyl group in NMR spectroscopy by equation: $f_{PMMA,NMR} = 1/(1 + 3/2 \times R \times M_{isobutylene}/M_{monomer})$. Reaction conditions: entry 6 of Table I.

Table III. Control Experiment without MMA for the Proof of BIIR's Degradation

Time (h)	$M_{n,control}$[a] $\times 10^{-5}$	$M_{n,corrected}$[b] $\times 10^{-5}$	$f_{PMMA,corrected}$[c]
0	2.68	2.68	0
1	0.51	0.87	0.41
3	0.34	1.42	0.76
5	0.38	2.00	0.81
7	0.35	2.33	0.85
9	0.35	2.93	0.88

[a] M_n based on MALLS using THF as eluent and PS as standards, dn/dc = 0.1353 (BIIR).
[b] $M_{n,corrected} = M_{n,control} + 60([M]_0/[I]_0) \times$ conversion $\times M_{monomer}$.
[c] The mass fraction of PMMA in the product of BIIR-*g*-PMMA. Reaction conditions: entry 6 of Table I without adding MMA.

RESULTS AND DISCUSSION

Graft Polymerization Initiated by BIIR Macroinitiator

The reaction conditions of graft polymerization of MMA from BIIR as a macromolecular initiator via ATRP approach were investigated by varying CuBr, $CuBr_2$ amount, and monomer concentration. The reaction time and conversion at different conditions are compared and listed in Table I. At a high concentration of catalyst (CuBr/PMDETA = 1/3,), gelation was observed only after reaction took place for 0.4 h (entries 1 and 4 of Table I), which might be caused by intermolecular coupling at a high instantaneous concentration of side-chain radical species in the presence of high catalyst concentration. To avoid this

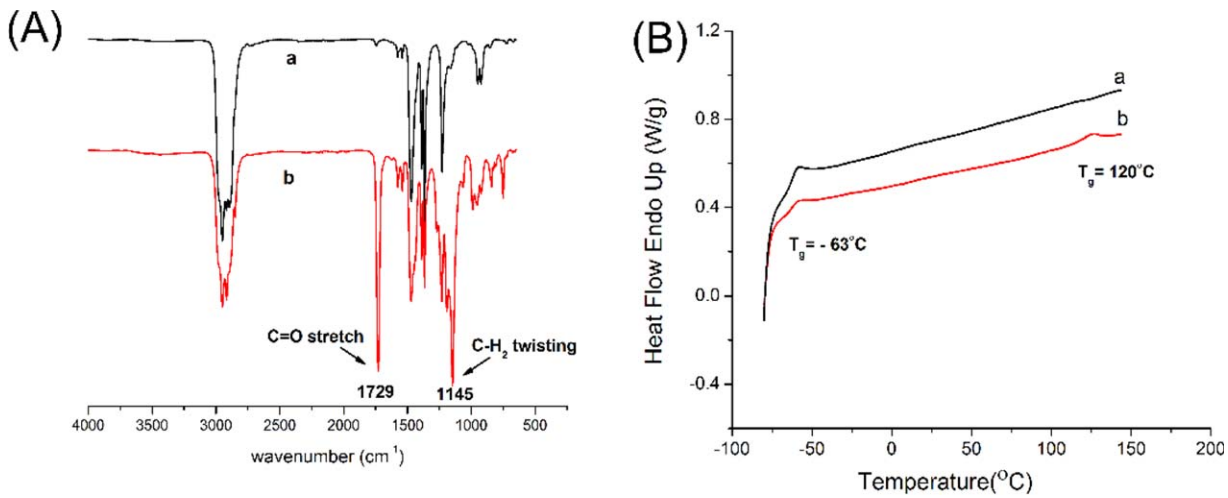

Figure 2. (A) ATR-FTIR spectra and (B) DSC thermogram of (a) BIIR and (b) BIIR-*g*-PMMA after 8 h of graft reaction. Reaction condition: entry 6 of Table I. [Color figure can be viewed in the online issue, which is available at wileyonlinelibrary.com.]

kind of *in situ* cross-linking by radical coupling, we added $CuBr_2$ as a deactivator to reduce the radical concentration and control the graft polymerization process. As compared with the reactions of entry 2 and entry 3 in Table I, the reaction conversion was reduced from 22.5% to 11.1%, indicating that the addition of $CuBr_2$ did slow down the reaction. Similar observation was reported by Tanaka's work.[33] By comparing the reactions of entry 1 vs entry 2, and entry 4 vs entry 5 in Table I, the reduction of activator CuBr content could avoid macroscopic gelation and maintain a relatively high conversion. In comparison with entry 1 of Table I, entry 6 showed that halving the monomer concentration could effectively avoid macroscopic gelation and obtain a higher monomer concentration as well. Thus, the reaction condition of entry 6 was used in the following experiments as an optimized condition.

A kinetic study on the reaction of entry 6 was carried out. A kinetic plot of $\ln([M_0]/[M])$ versus time is shown in Figure 1(a). A linear kinetic relationship between $\ln([M]_0/[M])$ with time was observed within the reaction time of 9 h, confirming the living characteristic of the system and a stable radical concentration was maintained during the polymerization.

GPC spectra are showed in Figure 1(b) and molecular weight parameters are summarized in Table II. Beyond our expectation, Figure 1(b) shows that all the peaks of resulting products appeared after that of pure BIIR, which means the M_n of graft copolymer is lower than that of pure BIIR (see detailed molecular weight parameters in Table II). But all GPC traces of graft products shifted toward higher molecular weight region as the reaction proceeded, without any peak due to inter- or intramolecular coupling reaction, and the peak from the BIIR macroinitiator completely disappeared. This may suggest that BIIR degraded during the polymerization which can be explained by that ATRP-generated radicals at the brominated isoprene mers abstracted hydrogen atoms at isobutylene mers while β scission easily took place for BIIR when free radical exists at isobutylene mers.[34] Similar results were obtained by Gillies *et al.*[24] that the decrease of M_n was ascribed to the interactions of the carboxylic acid groups with the column rather than the degradation of IIR backbones.

To confirm whether this degradation happened, we did a control experiment without using monomer MMA, and the results were summarized in Table III. The M_n of the resulting polymer decreased from 2.68×10^5 g/mol (0 h) to 0.51×10^5 g/mol (1 h) only in 1 h at 85°C in the presence of CuBr and PMDETA, and then stabilized at around 0.35×10^5 g/mol (3, 5, and 7 h). This means that macroinitiator BIIR indeed degraded and the major degradation process happened in the first hour of polymerization. Considering the degradation, the theoretical M_n of BIIR-*g*-PMMA in Table II should be corrected by subtracting the degradation part, and the corrected theoretical M_n and weight fraction of PMMA in the product of BIIR-*g*-PMMA are listed in the fourth and fifth columns of Table III, respectively. Compared with uncorrected theoretical M_n (fourth column of Table II), corrected theoretical M_n (fourth column of Table III) is much closer to the M_n obtained by GPC (fifth column of Table II). The molecular weight of PMMA fragments

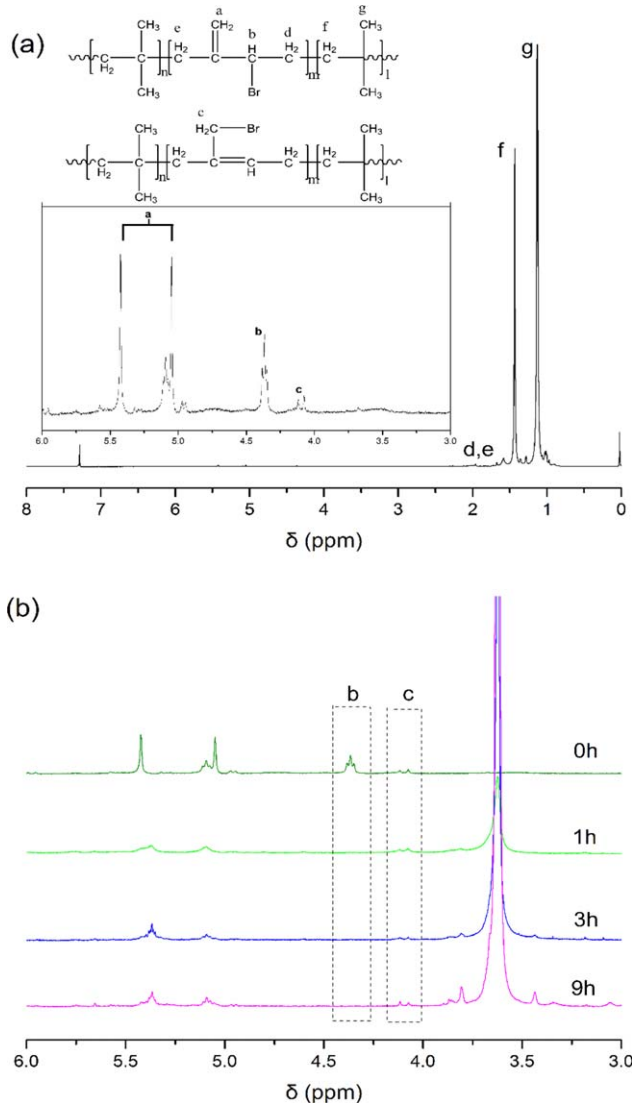

Figure 3. ^{1}H NMR spectra of (a) BIIR and (b) BIIR-*g*-PMMA of different graft reaction time in $CDCl_3$ (400 MHz, TMS standard). Reaction condition: entry 6 of Table I. [Color figure can be viewed in the online issue, which is available at wileyonlinelibrary.com.]

cannot be directly determined as the PMMA side chains cannot be cleaved using an acidolysis reaction, so the mass fraction of PMMA is estimated by taking the mass of BIIR out of the copolymer mass.

Structure Characterization of BIIR-*g*-PMMA

The FTIR spectra of BIIR and BIIR-*g*-PMMA are shown in Figure 2(A). The presence of the strong and narrow ester carbonyl peak at 1729 cm^{-1} confirms the presence of methyl methacrylate as well as the band at 1145 cm^{-1} attributed to the C—H twisting vibration of methylene group, which demonstrates successful grafting of MMA from BIIR macroinitiator.

The BIIR-*g*-PMMA copolymers were further characterized by ^{1}H NMR. The classification of each peak of BIIR's hydrogen in NMR spectrum is shown in Figure 3(a).28 As depicted in Figure 3(b), a new resonance at $\delta = 3.60$ ppm which is assigned to the

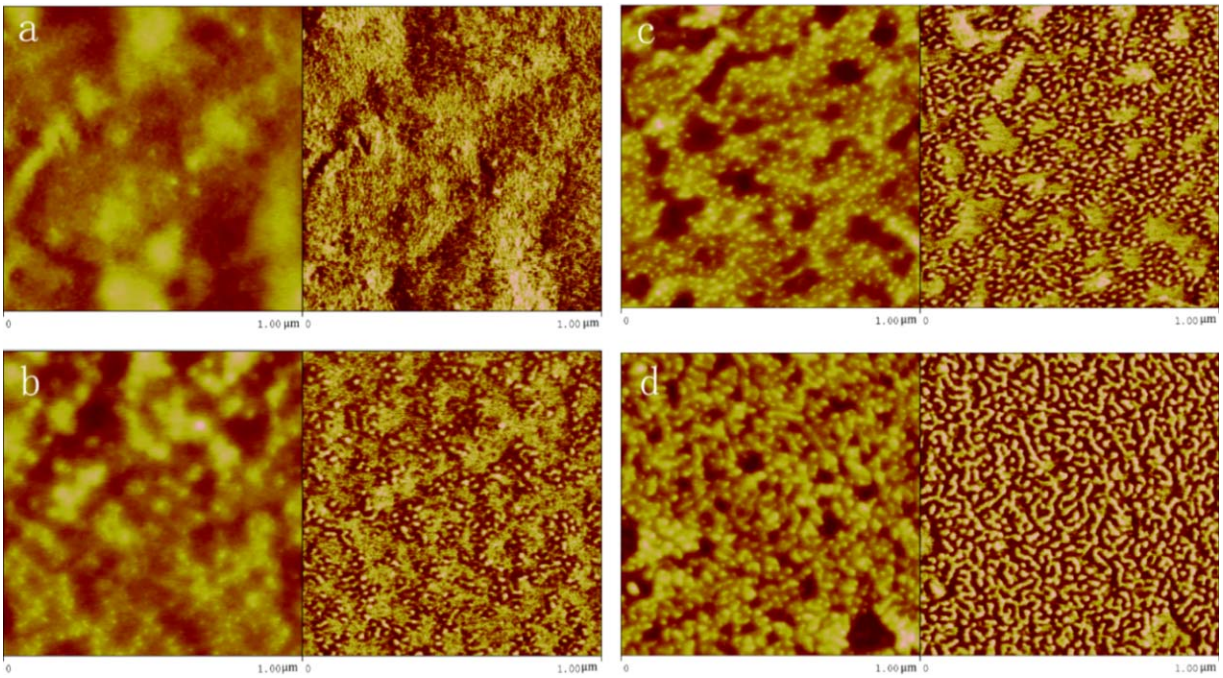

Figure 4. AFM images of thin films of BIIR (a) and BIIR-*g*-PMMA copolymers after (b) 5, (c) 7, and (d) 9 h of graft reaction followed by annealing in THF vapor for 24 h. Left: height image; right: phase contrast image. The vertical scale in all the height images is 10 nm. [Color figure can be viewed in the online issue, which is available at wileyonlinelibrary.com.]

methyl proton of -OCH_3 group in PMMA appeared and gradually increased, which demonstrates that graft polymerization of MMA from BIIR backbone progressed. Simultaneously, the resonance corresponding to the —CHBr— ($\delta = 4.34$ ppm) shifted to up field ($\delta = 3.10 \sim 3.08$ ppm). On the contrast, the chemical shifts of —CH_2Br ($\delta = 4.04$ and 4.08 ppm) still exit, which means secondary allylic bromine rather than primary allylic bromine in BIIR is the initiation site where MMA grafted from (see Scheme 1b). On one hand, secondary carbon radical is more stable than primary carbon radical; on the other hand, adjacent tertiary carbons bring about steric hindrance of secondary positions. For the two factors mentioned above, the former factor is predominant in this graft polymerization. This result is different from the conclusion of Parent *et al.*[8,26] that regioselective effect is predominant in the hydrogen atom abstraction from polyisobutylene by cumyloxy radicals. The low initiation efficiency may be another reason for the degradation of BIIR backbones, because of which not all ATRP-generated radicals at the brominated isoprene mers can initiate graft copolymerization of MMA in time; thus some ATRP-generated radicals may abstract hydrogen atoms at isobutylene mers and then cause β scission of isobutylene mers.

Degree of polymerization and mass fraction of PMMA in the product of BIIR-g-PMMA can be obtained by comparing integration of the PMMA and BIIR peaks in the H1 NMR (see detailed parameters in Table II). Comparing these against their gravimetric and GPC results, it can be found that DP_{NMR} and $f_{PMMA,NMR}$ are lower than DP_{theo} and $f_{PMMA,corrected}$ calculated by conversion and GPC results. This is because initiation efficiency cannot be 100% for BIIR and initiated sites per BIIR chain is not 60 any more caused by degradation.

Figure 2(B) shows the DSC curves of (a) BIIR and (b) BIIR-*g*-PMMA. In curve b, there are two steps at 120 and −63°C, respectively, indicative of the existence of two glass transition temperatures (T_g) in the graft copolymer. The existence of two T_gs is the hint of two phases in this polymer: a hard PMMA domain (high T_g) and a soft domain corresponding to the BIIR (low T_g). The appearance of two T_gs, along with spectroscopic results, is strong evidence for the success of the grafting polymerization.

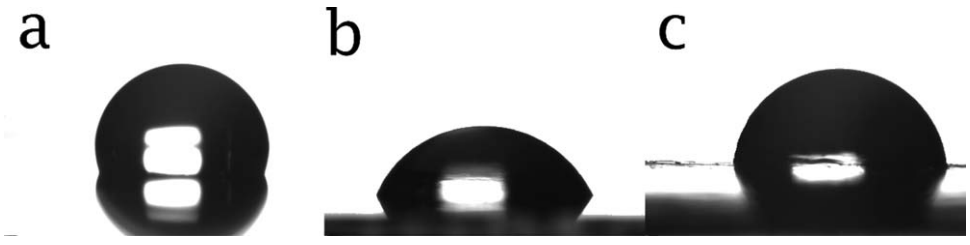

Figure 5. Water contact angles of (a) BIIR, (b) PMMA, and (c) BIIR-*g*-PMMA after 8 h of graft reaction. Reaction conditions: entry 6 of Table I.

AFM images can provide further information on morphology and structure of the graft copolymer, such as microphase separation and molecular size, including the length of main chain and side chains.[35,36] The two components of BIIR-*g*-PMMA (BIIR and PMMA) tend to be microphase separation because of the thermodynamic incompatibility.[37] As depicted in phase images, the stiff domain and the soft domain show bright and dark, respectively, in the tapping mode. From Figure 4(a), we can see the spin-cast film of pure BIIR shows a relatively flat and featureless surface as expected for a single phase. From Figure 4(b to c), as the weight fraction ($f_{PMMA,NMR}$) increases, the bright area increases from *ca* 18 to 22 nm. When $f_{PMMA,NMR}$ grows to 0.41 [Figure 4(d)], a worm-like morphology was observed. Therefore, the graft ratio and composition of the BIIR-g-PMMA copolymer determine the phase morphology.[38,39]

Water-contact angle measurement is a simple, quick, and effective method to examine the relative hydrophilicity of materials. Figure 5 shows the results of water-contact angles of BIIR and BIIR-g-PMMA surfaces. The water-contact angle on a BIIR-*g*-PMMA film was 83°, between those of BIIR (*ca* 109°) and pure PMMA film (*ca* 70°), suggesting the presence of BIIR and PMMA domains exposed to the film surface. Compared to BIIR, BIIR-*g*-PMMA copolymer has lower hydrophobicity due to the existence of grafted PMMA side chains. The results further support the successful grafting reactions of PMMA from BIIR macromolecular chains.

CONCLUSIONS

Commercial BIIR rubber is generally made by brominating with liquid bromine rather than expensive bromination reagents. The allylic bromine atoms on the macromolecular chains of BIIR were first utilized as a macromolecular initiator for graft polymerization of MMA via an ATRP method. The polymerization conditions were optimized to suppress macroscopic gelation occurred during the polymerization and improve the monomer conversion by adjusting the catalyst and monomer concentration. A lower monomer concentration can effectively avoid gelation and lead to a higher monomer concentration. ATR-FTIR, NMR spectroscopic results, along with two T_gs of DSC, microphase separation of AFM and hydrophobicity of the copolymer surface, have provided strong evidence for the success of the grafting polymerization. This study unveils that commercial products can be directly used for ATRP reactions to make new polymers and broadens the sustainable application of butyl rubber, potentially as highly efficient compatibilizer in immiscible polymer blends.

ACKNOWLEDGMENTS

The authors would like to acknowledge the financial support from Lanxess Company and the National Natural Science Foundation of China (grant numbers 51273109 and 51235008), and be grateful for the discussion with Dr Sharon Guo and Dr Steven Gao in Lanxess Company. The authors also thank the staff of Instrumental Analysis Center of Shanghai Jiao Tong University for the measurements.

REFERENCES

1. Chu, C. Y.; Vukov, R. *Macromolecules* **1985**, *18*, 1423.
2. Faba, M. A. J.; Parent, J. S.; Whitney, R. A. *Ind. Eng. Chem. Res.* **2011**, *50*, 680.
3. Takahashi, S.; Goldberg, H. A.; Feeney, C. A.; Karim, D. P.; Farrell, M.; O'Leary, K.; Paul, D. R. *Polymer* **2006**, *47*, 3083.
4. Parent, J. S.; White, G. D. F.; Thom, D. J.; Whitney, R. A.; Hopkins, W. *J. Polym. Sci. Polym. Chem.* **2003**, *41*, 1915.
5. Xu, W.; Cheng, Z.; Zhang, Z.; Zhang, L.; Zhu, X. *React. Funct. Polym.* **2011**, *71*, 634.
6. Wang, X. S.; Luo, N.; Ying, S. K. *Polymer* **1999**, *40*, 4515.
7. Feng, Y.; Wang, Y. X.; Shao, H. Q.; Zhang, E. H.; Wang, Z.; Zhao, J. R. *J. Ind. Eng. Chem.* **2014**, *20*, 184.
8. Dakin, J. M.; Shanmugam, K. V. S.; Twigg, C.; Whitney, R. A.; Parent, J. S. *J. Polym. Sci. A Polym. Chem.* **2015**, *53*, 123.
9. Otsu, T.; Yoshida, M. *Die Makromolekulare Chemie, Rapid Commun.* **1982**, *3*, 127.
10. Georges, M. K. *Macromolecules* **1993**, *26*, 2987.
11. Chiefari, J.; Chong, Y. K.; Ercole, F.; Krstina, J.; Jeffery, J.; Le, T. P. T.; Mayadunne, R. T. A.; Meijs, G. F.; Moad, C. L.; Moad, G.; Rizzardo, E.; Thang, S. H. *Macromolecules* **1998**, *31*, 5559.
12. Wang, J. S.; Matyjaszewski, K. *J. Am. Chem. Soc.* **1995**, *117*, 5614.
13. Coffin, R. C. *J. Am. Chem. Soc.* **2010**, *132*, 13869.
14. Li, M.; Zhang, L.; Tao, M.; Cheng, Z.; Zhu, X. *Polym. Chem.* **2014**, *5*, 4076.
15. Shi, Y.; Zhu, W.; Chen, Y. *Macromolecules* **2013**, *46*, 2391.
16. Wang, Z.; Zhang, Y.; Jiang, F.; Fang, H.; Wang, Z. *Polym. Chem.* **2014**, *5*, 3379.
17. Bolton, J. *ACS Macro Lett.* **2012**, *1*, 15.
18. Xu, G.; Wang, D.; Buchmeiser, M. R. *Macromol. Rapid Commun.* **2012**, *33*, 75.
19. Zhang, B.; Wepf, R.; Fischer, K.; Schmidt, M.; Besse, S.; Lindner, P.; King, B. T.; Sigel, R.; Schurtenberger, P.; Talmon, Y.; Ding, Y.; Kroger, M.; Halperin, A.; Schluter, A. D. *Angewandte Chemie* **2011**, *50*, 737.
20. Xia, Y.; Kornfield, J. A.; Grubbs, R. H. *Macromolecules* **2009**, *42*, 3761.
21. Sun, J. P.; Hu, J. W.; Liu, G. J.; Xiao, D. S.; He, G. P.; Lu, R. F. *J. Polym. Sci. Polym. Chem.* **2011**, *49*, 1282.
22. Gao, H. F.; Matyjaszewski, K. *J. Am. Chem. Soc.* **2007**, *129*, 6633.
23. Matyjaszewski, K. *Macromolecules* **2012**, *45*, 4015.
24. McEachran, M. J.; Trant, J. F.; Sran, I.; de Bruyn, J. R.; Gillies, E. R. *Ind. Eng. Chem. Res.* **2015**, *54*, 4763.
25. Truelsen, J. H.; Kops, J.; Batsberg, W. *Macromol. Rapid Commun.* **2000**, *21*, 98.
26. Parent, J. S.; Thom, D. J.; White, G.; Whitney, R. A.; Hopkins, W. *J. Polym. Sci. A Polym. Chem.* **2001**, *39*, 2019.
27. Gardner, I. J.; Plains, S.; Fusco, J. V. U.S. Patent 4649178 1987.
28. Cheng, D. M.; Gardner, I. J.; Wang, H. C.; Frederick, C. B.; Dekmezian, A. H.; Hous, P. *Rubber Chem. Technol.* **1990**, *63*, 265.

29. Kaszas, G. *Rubber Chem. Technol.* **2000**, *73*, 356.
30. Jakubowski, W.; Tsarevsky, N. V.; Higashihara, T.; Faust, R.; Matyjaszewski, K. *Macromolecules* **2008**, *41*, 2318.
31. Liu, X.; Tian, Z.; Chen, C.; Allcock, H. R. *Macromolecules* **2012**, *45*, 1417.
32. Li, W.; Gao, H.; Matyjaszewski, K. *Macromolecules* **2009**, *42*, 927.
33. Tanaka, K.; Matyjaszewski, K. *Macromolecules* **2007**, *40*, 5255.
34. Loan, L. D. *J. Polym. Sci. A* **1964**, *2*, 2127.
35. Sriprom, W.; James, M.; Perrier, S.; Neto, C. *Macromolecules* **2009**, *42*, 3138.
36. Lee, H.; Matyjaszewski, K.; Yu-Su, S.; Sheiko, S. S. *Macromolecules* **2008**, *41*, 6073.
37. Brandrup, J. A. I. H. Polymer Handbook, 3rd ed.; John-Wiley: NewYork, **1989**.
38. Sheiko, S. S.; Möller, M. *Chem. Rev.* **2001**, *101*, 4099.
39. Lee, H.; Jakubowski, W.; Matyjaszewski, K.; Yu, S.; Sheiko, S. S. *Macromolecules* **2006**, *39*, 4983.